Melittin-Induced Changes of the Macroscopic Structure of Phosphatidylethanolamines†

A. M. Batenburg,*,‡ J. H. van Esch,‡ and B. de Kruijff§

Department of Biochemistry and Institute of Molecular Biology and Medical Biotechnology, State University of Utrecht, Padualaan 8, (De Uithof) Utrecht, The Netherlands

Received August 26, 1987; Revised Manuscript Received November 16, 1987

ABSTRACT: The binding of melittin to phosphatidylethanolamine model systems and its influence on the supramolecular organization of the lipid were investigated with binding assays, differential scanning calorimetry, ^{31}P NMR, freeze–fracture electron microscopy, and small-angle X-ray scattering. The results are compared with binding to an analogous phosphatidylcholine and structural consequences thereof. Melittin binds with similar affinity to both lipid types in the liquid-crystalline state; at gel-phase temperatures, in contrast, interaction with phosphatidylethanolamine is much weaker and does not lead to the bilayer fragmentation observed for phosphatidylcholines. With regard to phosphatidylethanolamine polymorphism, it is shown that melittin acts as an inhibitor of H_{II}-phase formation and as a stabilizer of the bilayer organization. It is demonstrated that the remarkable variety of effects of melittin on the polymorphism of different membrane phospholipids can be understood in a relatively simple concept, taking into account the relative position and the shape of the interacting components.

Melittin, a 26 amino acid long, basic and hydrophobic peptide, is the main proteinaceous constituent of the venom of the honeybee. Due to the amphiphilicity of its sequence with most charges concentrated at the C-terminus, the peptide interacts with biological and pure lipid membranes [see Habermann (1972) and Dufourcq et al. (1984) and references cited therein] and has therefore been extensively studied as a model peptide for peptide–lipid interactions.

It has been shown that the structure of both the peptide and the lipid component is affected by melittin–phospholipid interactions. The peptide secondary structure exhibits a change from an almost complete random coil to ±70% α-helix (Vogel, 1981). A comparable amount of helical structure is found for melittin free in solution at high concentration and high ionic strength (Bello et al., 1982) where the peptide forms tetramers in which the hydrophobic sites are thought to be shielded from the aqueous surrounding, analogous to the structure in melittin crystals (Terwillinger & Eisenberg, 1982).

In spite of the preference for negatively charged lipids (Dufourcq & Faucon, 1977), most studies of melittin influence on lipid molecular properties were restricted to phosphatidylcholines. Fluorescence depolarization experiments and Raman spectroscopy pointed to a slight increase of order above the gel to liquid-crystalline transition and a distinct decrease of order at gel-phase temperature (Lavialle et al., 1980; Dasseux et al., 1984); the enthalpy of the main transition was decreased such that at low peptide:lipid ratios 1 melittin molecule prevents the cooperative transition of about 10 phosphatidylcholine molecules (Mollay, 1976), without affecting to a large extent the transition temperature (Mollay, 1976; Dasseux et al., 1984).

Polypeptides, however, in principle are also able to modulate the supramolecular organization of phospholipids by induction of nonbilayer structures, as reviewed in De Kruijff et al., (1985b). Melittin influence on lipid polymorphism is of particular interest, since its structure resembles the presequences of mitochondrion-destined proteins and pro- and eucaryotic signal peptides (Von Heijne et al., 1985), found to be essential for membrane passage.

The action of melittin on lipid morphology appears to be rather complex. After early negative-stain electron microscopic observations of bilayer fragmentation in phosphatidylcholine systems (Sessa et al., 1969) and descriptions of clearance of lipid dispersions (Lavialle et al., 1980), more sophisticated structural studies demonstrated the formation of discoid structures, interpreted as flat bilayer fragments surrounded by a belt of amphipathic melittin helices (Prendergast et al., 1982; Freer et al., 1984). These structures appeared to be specific for gel-phase phosphatidylcholines; in the liquid-crystalline phase, instead a vesicularization of multilamellar structures was observed (Dufourc et al., 1986). At peptide:lipid molar ratios higher than 1:5 finally, irrespective of the physical state of the pure lipid at the temperature in question, still smaller, micellar structures are formed (Dufourcq et al., 1986). On the basis of these findings, melittin is often considered as a detergent on a peptide base. In dispersions of the favored negatively charged phospholipids, however, melittin, instead of solubilizing the lipid material, induced an increase of turbidity and at high peptide:lipid ratio a precipitation of the lipid. Further structural characterization indicated the formation of inverted types of lipid structure in cardiolipin (Batenburg et al., 1987a) and in other negatively charged phospholipids (Batenburg et al., 1987c). According to the shape–structure concept of lipid polymorphism (Cullis & De Kruijff, 1979), the effects on phosphatidylcholines and on negative phospholipids are exactly opposing features, and an attempt was made to reconcile these results on the basis of a different type of insertion of the peptide (Batenburg et al., 1987b).

In this study, we report on the structural alterations induced by melittin in a third major class of membrane phospholipids, the phosphatidylethanolamines. The naturally occurring unsaturated representatives of this lipid type, unlike their phosphatidylcholine counterparts, do not adopt a bilayer organization upon hydration at physiological temperatures but

† The investigations were carried out under the auspices of the Netherlands Foundation for Chemical Research (SON) and with financial aid from the Netherlands Organization for the Advancement of Pure Research (ZWO).

* Correspondence should be addressed to this author.

‡ Department of Biochemistry.

§ Institute of Molecular Biology and Medical Biotechnology.

0006-2960/88/0427-2324$01.50/0

instead form an inverted hexagonal structure, the H_{II} phase (Cullis & De Kruijff, 1979). It is shown in comparative experiments that at gel-phase temperatures the interaction of melittin with dielaidoylphosphatidylethanolamine (DEPE)[1] is weaker than that with DEPC, not leading to fragmentation of the bilayers. Most important, however, the peptide was found to stabilize bilayer structure at H_{II}-phase temperature, both in DOPE and in DEPE. These results, which emphasize the unique lipid structure modulating activity of melittin, can be rationalized in terms of the shape structure concept of polymorphism extended toward peptide–lipid systems.

Materials and Methods

Materials. DEPC and DOPC were synthesized as described before (Van Deenen & De Haas, 1964). Their conversion to DEPE and DOPE was also reported earlier (Comfurius & Zwaal, 1977); their purity was checked by thin-layer chromatography. Melittin from commercial sources (Serva and Sigma) was found to be of insufficient purity and was therefore isolated from whole bee venom (Serva) by crude fractionation over Sephadex G-50 (King et al., 1976) and freed from phospholipase traces by a covalent chromatography based method using thiopropyl-Sepharose 6B (Pharmacia) (Batenburg et al., 1987b). No lipid degradation was observed after a 24-h incubation of egg PC with melittin at a lipid:melittin ratio $R_i = 4$ at 40 °C in the presence of 10 mM $CaCl_2$. All other chemicals were of analytical grade or better.

Model Membranes, Sample Preparation, and Routine Procedures. Phospholipid dispersions were obtained by hydration at L_α temperatures of a lipid film dried from chloroform. Since PEs usually form very large multilamellar aggregates instead of homogeneous dispersions, melittin was always introduced via the "internal method", i.e., dissolved in the buffer used to disperse the lipid, to improve sample homogeneity. The pH of the samples thus obtained was not measurably influenced by the presence of the peptide, not even in the most concentrated samples used for DSC.

PC SUV were used only in fluorescence experiments; they were prepared from lipid dispersions by sonication with a Branson B12 sonifier equipped with a 0.5-in. flat-top disruptor tip under nitrogen in ice–water applying 50 W for 10 times 30 s, and were isolated as the supernatant of a 10 min, 27000*g* centrifugation. In all experiments, a buffer was used containing 25 mM Pipes, 100 mM NaCl, and 1 mM EDTA, pH 7.3. Phospholipid was determined after destruction with 70% perchloric acid (Fiske & Subbarow, 1925; Rouser et al., 1975).

Binding Experiments. Approximately 600 nmol of lipid was dispersed in 1.5 mL of buffer containing varying amounts of melittin. After being cooled to the appropriate temperature and a 60-min incubation, "bound" and "unbound" peptides were separated by a 30 min, 27000*g* centrifugation at 4 °C. The amounts of lipid and peptide remaining in the supernatant and the amount of lipid pelleted were determined, the peptide on the basis of its fluorescence after a 5-fold dilution in methanol (λ_{ex} = 280 nm, λ_{em} = 330 nm). The data were analyzed with a computer program which, by means of iterative nonlinear regression, calculates the stoichiometry and dissociation constant (K_D), using the equation $K_D = [P][L][PL_N]^{-1}$ where [P] and $[L_N]$ represent the concentrations of free peptide and free peptide binding sites, respectively (Hille et al., 1981).

Intrinsic Fluorescence Measurements. Changes of the intrinsic tryptophan fluorescence of melittin upon lipid binding were followed by titration of a 10 μM melittin solution with SUV; 3 min after each addition, an emission spectrum was recorded with a Perkin-Elmer MPF 3 fluorometer. Alternatively, separate samples with varying lipid content were prepared by using the above-mentioned "internal method", in which no sonication step was included. The shift of the wavelength of maximal fluorescence was analyzed as described above.

Differential Scanning Calorimetry. For DSC, 10 μmol of lipid was dispersed in 100 μL of buffer and without concentration steps transferred into stainless-steel sample pans. DSC was carried out with a scan rate of 2 °C/min on a Perkin-Elmer DSC-4 calorimeter equipped with a Perkin-Elmer thermal analysis data station; DEPE samples were kept at L_α-phase temperatures for 30 min before passing through the L_α–H_{II} transition. The instrument was calibrated with an indium standard. Afterward, the exact amount of lipid present in the pans was determined after the samples were dissolved in 1:1 methanol/chloroform (v/v).

Phosphorus NMR. ^{31}P NMR experiments were performed at 121.5 MHz with a Bruker MSL 300, applying broad-band decoupling as described before (Chupin et al., 1987). One-milliliter samples containing 10–30 μmol of lipid and prepared as described above were, depending on the amount of lipid, subjected to 5000–30000 45° pulses with a 1-s interpulse time; a 75-Hz line broadening was introduced to suppress the noise. For each lipid:peptide ratio (R_i), separate samples were prepared at L_α-phase temperatures.

Small-Angle X-ray Scattering. Samples were transferred into 0.5 × 1.5 × 16 mm slits of the sample holders, protected against drying with cellophane, and irradiated for 30 min with a 1 × 0.2 mm copper K_α beam (40 kV, 20 mA) in a Kratky camera with a position-sensitive LETI detector, interphased to a microcomputer.

Freeze–Fracture Electron Microscopy. Freeze–fracturing was performed on similar samples after plunge freezing with a Reichert Jung KF80 (Sitte et al., 1987) without the use of cryoprotectants. Replicas were analyzed with a Philips 420 microscope.

Results

Binding to Liquid-Crystalline DEPE and DEPC. For comparative studies of melittin binding to PEs and PCs, the dielaidoyl species were chosen on the basis of their favorable gel–liquid-crystalline-phase transitions around 40 and 14 °C, respectively (Van Dijck et al., 1976). Hydration at L_α-phase temperature of DEPE in the presence of melittin up to R_i = 30 resulted in visually homogeneous dispersions, which were not suited for centrifugation-based binding experiments, because of incomplete pelleting at low R_i, but which were suited for fluorescence measurements. The wavelength of maximal fluorescence is shown in Figure 1 as a function of R_i; in order to compare with literature data, DEPC was also stepwise added to melittin in the form of SUV, resulting in essentially the same fluorescence–R_i correlation (Figure 1B). The formation of micellar structures, for PC–melittin known to exist at very low R_i values (Dufourcq et al., 1986), was not reflected in the fluorescence shift measurements which obeyed simple saturation kinetics. The results of the data analysis are compared in Table I, from which it is clear that both stoichiometry and affinity are similar for binding of melittin to the two lipid systems in the liquid-crystalline state.

[1] Abbreviations: DSC, differential scanning calorimetry; PC, phosphatidylcholine; PE, phosphatidylethanolamine; DEPC, dielaidoyl-PC; DEPE, dielaidoyl-PE; DOPE, dioleoyl-PE; DPPC, dipalmitoyl-PC; R_i, phospholipid:peptide molar ratio; SUV, small unilamellar vesicle(s); EDTA, ethylenediaminetetraacetic acid; Pipes, piperazine-*N*,*N*′-bis(2-ethanesulfonic acid).

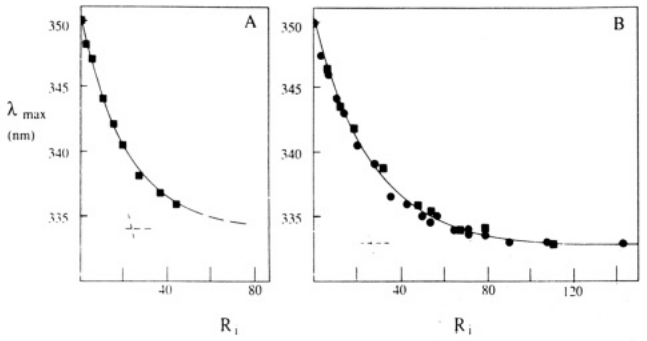

FIGURE 1: Wavelength of maximal fluorescence of the melittin tryptophan as a function of the applied lipid:melittin ratio. (A) Results for DEPE (50 °C) and (B) for DEPC (25 °C). (■) Samples prepared according to the "internal method"; (●) results of titration of melittin with SUV. Experimental details are given under Materials and Methods; excitation wavelength, 280 nm. The crosses in the lower left corner indicate the stoichiometry.

Table I: Stoichiometries and Dissociation Constants for Binding of Melittin to DEPE and DEPC

lipid	temp (°C) [physical state]	method[a]	$\Delta\lambda_{max}$[b] (nm)	N[c]	K_D[d] (μM)
DEPE	50[L_α]	F	16	24.4 ± 1.3	1.7 ± 0.8
DEPC	25[L_α]	F	17	24.8 ± 1.2	1.5 ± 0.2
DEPE	25[L_β]	C		39.3 ± 1.3	7.6 ± 0.7
DEPC	5[L_β]	F	20	60 ± 4	0.11 ± 0.04

[a] F = fluorescence assay, C = centrifugation-based assay. [b] Final shift of the wavelength of maximal tryptophan fluorescence. [c] Number of lipids forming one peptide binding site. [d] K_D = dissociation constant, as defined under Materials and Methods.

Binding to DEPE and DEPC at Gel-Phase Temperatures. When DEPE–melittin samples were cooled to 25 °C, precipitation occurred, in contrast to the DEPC samples showing clearance of the dispersion upon cooling to L_β temperature at $R_i < 25$. Fluorescence experiments were therefore impossible. On the other hand, a complete pelleting of the PE was observed upon centrifugation at all R_i values, enabling direct binding studies to be performed on the basis of separation of bound and unbound peptide by centrifugation (Figure 2A). Analysis of the data (Table I) indicates a stoichiometry of 40 lipids forming 1 melittin binding site and an affinity which is markedly lower than at temperatures above the transition.

In comparative experiments with DEPC, from $R_i = 100$ onward a detectable amount of lipid phosphorus was found in the supernatant. Down to $R_i = 20$, the lipid:peptide molar ratio in the supernatant remains constant at 24 ± 2 (Figure 2B, insert), in agreement with the ratio found for the disklike structures observed in melittin–DPPC systems in the gel phase (Dufourcq et al., 1986). Due to this solubilization of the lipid, the maximal amount of melittin that can bind to large structures of DEPC cannot be calculated from Figure 2B, but it is clear from the slope of the binding curve at low peptide concentration that the affinity of melittin for PC is considerably higher than for PE. The same can be concluded from intrinsic fluorescence measurements (Figure 3); the data analysis (Table I), however, cannot be directly compared to the values for PE or for PC at L_α temperatures, since the fluorescence change here reflects binding both to large structures and also in disklike aggregates for which by measurements at high R_i after centrifugation an 8-nm shifted fluorescence maximum could be estimated.

Influence on the Phase Transitions of DEPE. DSC was used to study the influence of melittin on the thermotropic behavior of DEPE and DEPC. No concentration step was included in the sample preparation in order to avoid problems related to partial solubilization of the lipid and differential binding of melittin above and below the phase transition (see above). The concentrations used in these experiments as well as in those of following paragraphs is such that over 99% of the melittin present is expected to be bound on the basis of the determined K_D's, irrespective of the lipid physical state.

With respect to the main transition, Figure 4 shows that the presence of melittin in DEPE samples results in the rise

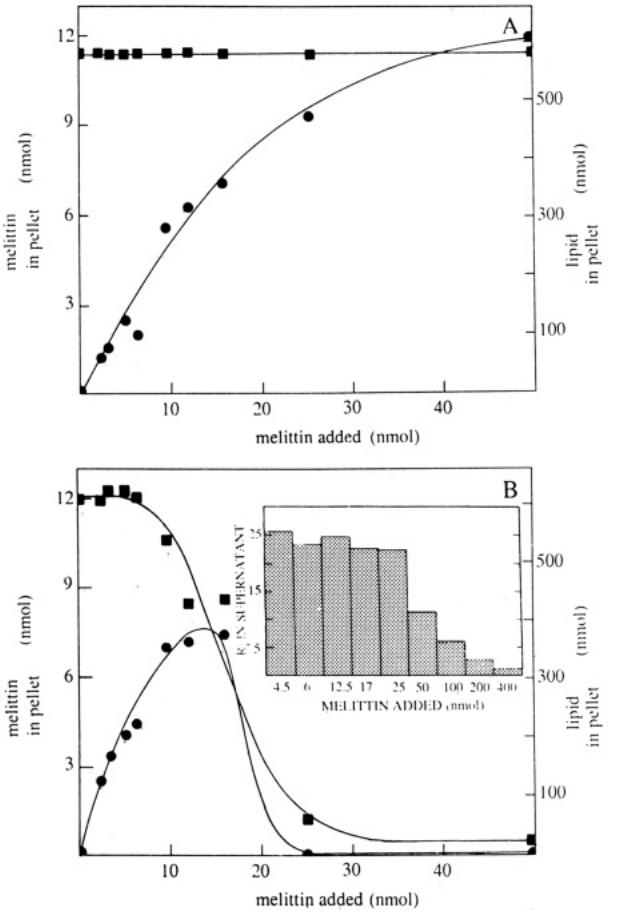

FIGURE 2: Binding of melittin to DEPE (A) and DEPC (B) as measured with the centrifugation-based assay (see Materials and Methods). (■) Lipid recovered in the pellet; (●) melittin bound to the pelleted lipid; 580 nmol of PE or 600 nmol of PC was present; total volume 1.5 mL. The insert shows the lipid:melittin ratio determined in the supernatant versus the initial amount of peptide; data points at lower R_i are also included.

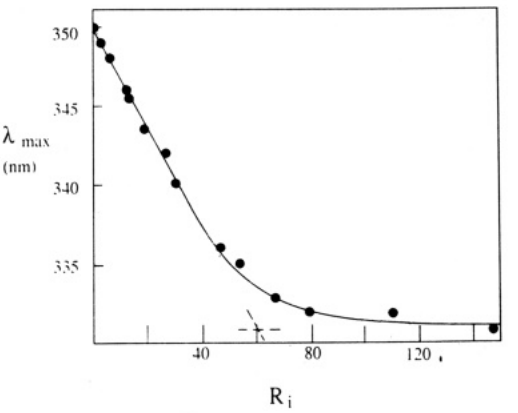

FIGURE 3: Wavelength of maximal tryptophan fluorescence as a function of the applied DEPC:melittin ratio at 5 °C. The "internal method" of sample preparation and measurement is outlined under Materials and Methods; excitation wavelength, 280 nm. The cross at the bottom of the figure indicates the stoichiometry.

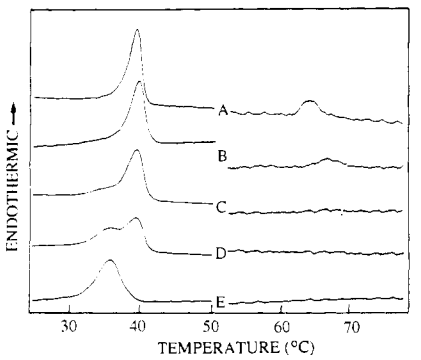

FIGURE 4: Thermograms of DEPE in the presence of various amounts of melittin. Pure lipid (A), R_i = 120 (B), R_i = 80 (C), R_i = 40 (D), R_i = 20 (E). For the 55–75 °C trajectory, the y scale is 3 times expanded. The experimental conditions are described under Materials and Methods.

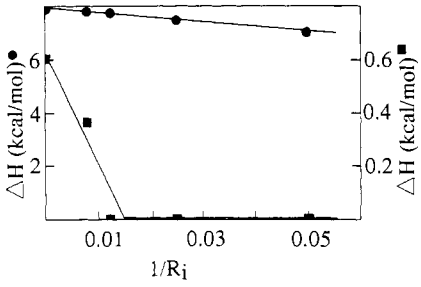

FIGURE 5: Enthalpy of the L_β–L_α (●) and L_α–H_{II} (■) transition of DEPE as a function of the applied melittin:lipid ratio. The uncertainty in the data points is approximately 0.2 kcal/mol.

of a new transition at about 4 °C lower temperature than the original transition, the disappearance of which is completed at R_i = 20. Scans are reversible upon cooling to L_β temperature and direct subsequent reheating, but not unexpected on the basis of the foregoing, changes occur upon longer storage at low temperatures. These were not further analyzed. The appearance of a discrete new cooperative transition suggests the existence of a structural separation between lipid domains rich in melittin and unaffected, peptide-poor regions. The shift is accompanied by a slight, linear decrease of total transition enthalpy (Figure 5). For phosphatidylcholines, larger effects on the enthalpy content have been reported (Mollay, 1976; Dasseux et al., 1984); control experiments confirmed these for DEPC (17% decrease at R_i = 50) and showed a minor (1.5 °C at R_i = 20) shift to higher instead of lower temperature (data not shown).

The effect of melittin on the bilayer–H_{II} transition at 63 °C appears to be much larger. Already at R_i = 80, no endotherm can be detected anymore, indicating either that no transition takes place or, alternatively, that its cooperativity is lost. This question was tackled by lipid structure-probing techniques.

Effects on the Supramolecular Structure of DEPE and DEPC. First, the melittin–DEPC system was studied to allow a comparison between our observations on PE and literature data on PC. Samples were prepared via the internal method. In the absence of melittin, ^{31}P NMR shows at 25 °C a spectrum with a high-field peak and a low-field shoulder and a residual chemical shift anisotropy $\Delta\sigma$ = 44 ppm, attributable to phospholipids experiencing rapid long-axis rotation in extended bilayers (Seelig, 1978), which from now on will be referred to as the "bilayer spectrum" (Figure 6). At R_i = 20, the main features of the bilayer spectrum are conserved, yet the less defined line shape and decreased $\Delta\sigma$ of 42 ppm point to a higher degree of curvature and are consistent with the vesicularization process described for DPPC (Dufourcq et al., 1986). Increasing the relative amount of melittin results in a conversion of the bilayer spectrum to a sharp isotropic signal, in line with the DPPC results consistent with micelle formation. If the samples are cooled to gel-phase temperature (Figure 6 upper panels), the effect of melittin at R_i = 20 is more drastic: the broad bilayer spectrum ($\Delta\sigma$ = 54 ppm), typical for the L_β phase (De Kruijff et al., 1985a), already at this stage is replaced by an isotropic signal, in perfect agreement with the solubilization observed earlier and with the disk formation reported for other gel-phase PCs at this ratio (Dufourcq et al., 1986). As judged from the signal width, at lower R_i still smaller, most likely micellar, structures are formed.

The ^{31}P NMR spectrum of gel-phase DEPE, in contrast, shows absolutely no influence of the presence of melittin at R_i = 20 (cf. Figure 7A,B). At fluid-phase temperature, ^{31}P NMR shows a signal at +11 ppm which we interpret as a "bilayer" type of signal with reduced low-field shoulder intensity, suggesting magnetic orientation of the melittin-containing bilayers (Seelig et al., 1985); the chemical shift anisotropy is then distinctly reduced from 40 to 32 ppm. In addition, a small amount of lipid shows isotropic motion (peak at 0 ppm). More dramatic effects of melittin are observed at 65 °C. Whereas the pure lipid has completely adopted the H_{II} phase, characterized by a ^{31}P NMR spectrum of strongly reduced $\Delta\sigma$ and a reversed asymmetry, in the melittin–DEPE sample, no H_{II} phase is observed, and a large fraction of the lipid remains organized in extended bilayers; the rest of the lipid phosphates give rise to a broad isotropic signal. At still higher temperature, all lipids give rise to an isotropic signal, and the spectrum recorded after cooling to 50 °C indicates that the formation of the structure underlying this signal is not readily reversible; yet, upon cooling to 25 °C, the normal gel-phase spectrum again appears (data not shown).

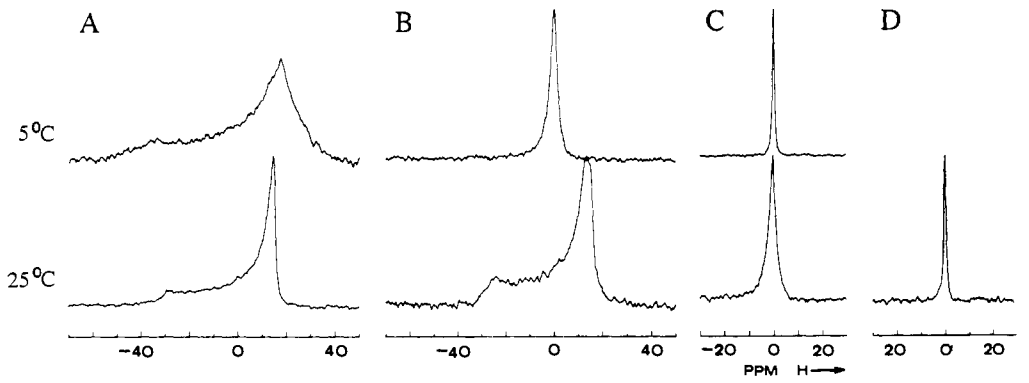

FIGURE 6: 121.5-MHz ^{31}P NMR spectra of DEPC in the presence of melittin. (A) Pure lipid; (B) R_i = 20; (C) R_i = 5; (D) R_i = 2. 0 ppm reflects the position of the signal of lysophosphatidylcholine micelles.

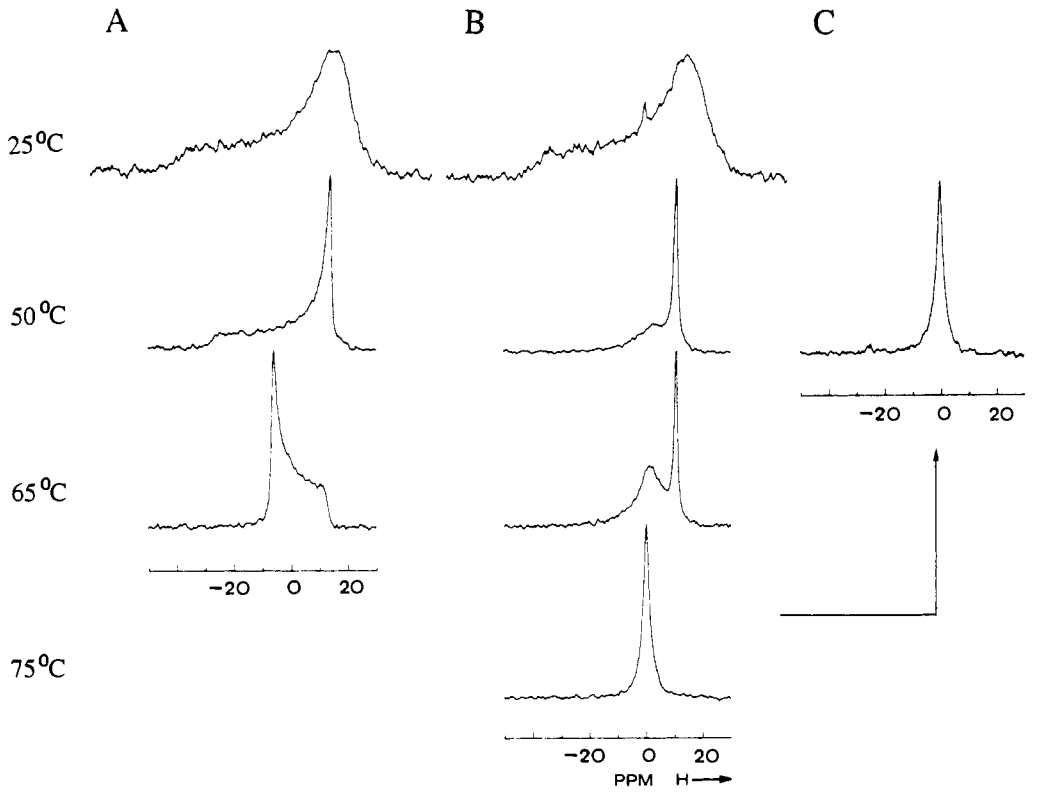

FIGURE 7: 121.5-MHz ^{31}P NMR spectra of (A) pure DEPE and (B) DEPE hydrated with melittin (R_i = 20). Spectrum C was recorded for the melittin-containing sample after heating to 75 °C and subsequent cooling to 50 °C.

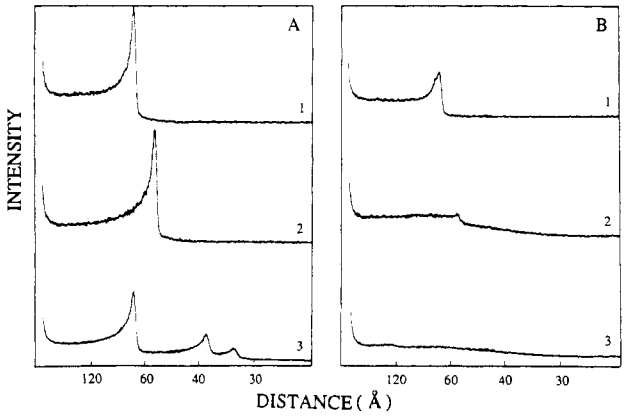

FIGURE 8: Small-angle X-ray scattering of DEPE samples in the absence (A) and presence (B) of melittin (R_i = 20) at 25 °C (1), 50 °C (2), and 70 °C (3).

Small-angle X-ray scattering (Figure 8) confirms the lack of structural effects of melittin on DEPE in the gel phase. Independent of the presence of the peptide, the sharp reflection indicates a repeat distance for the stacked bilayers of 66.5 Å; the absence of second or higher order reflections is common to PE bilayer systems (Valtersson et al., 1985). In the L_α phase, the first-order reflection at 54.7 Å is almost completely abolished in the presence of melittin at R_i = 20, indicating that melittin inhibits regular bilayer stacking at this temperature. At 70 °C, the $1:(1/3^{1/2}):(1/2)$ spacings of an H_{II} phase with 76.4-Å tube diameter are observed in the pure lipid sample; the melittin-containing sample does not show this diffraction pattern, confirming the complete absence of H_{II} phase, nor does it reveal any other sharp reflections, indicating that the isotropic ^{31}P NMR signal reflects no regularly stacked, for instance cubic, structure.

Freeze–fracture replicas of melittin–DEPE samples, obtained after quenching from ambient, gel-phase temperature, visualize extended smooth bilayers, contrasting the electron microscopic observations on systems of melittin with gel-phase PCs (Dufourc et al., 1986), and confirm the regular stacking deduced from the small-angle X-ray pattern. Unfortunately, freeze–fracture cannot be used to gain insight in the morphology of the structure adopted by melittin–DEPE complexes at temperatures around 75 °C, giving rise to the isotropic ^{31}P NMR signal, since quenching from such a high temperature does not guarantee conservation of structure. This was one of the reasons to study the influence of melittin on PE polymorphism in more detail using DOPE, which shows an L_α–H_{II} transition at a more favorable temperature.

Effect on the Polymorphism of DOPE. Figure 9 shows the ^{31}P NMR spectra of DOPE samples with increasing melittin content, both below and above the L_α–H_{II} transition. Pure DOPE shows at 2 °C a bilayer spectrum with $\Delta\sigma$ = 43 ppm and at 15 °C a spectrum typical for the H_{II} phase. The presence of melittin (R_i = 120) leads at 2 °C to a broadened type of line shape, reflecting increased motional averaging of the lipid molecules (Burnell et al., 1980), whereas at 15 °C superimposed on the H_{II} spectrum an isotropic signal is observed, the contribution of which slightly increases with temperature. Upon being cooled to 2 °C, the samples show considerable hysteresis. At R_i = 40, the contribution of the isotropic component is further increased.

Most important, however, at R_i = 20 (Figure 9D), melittin not only inhibits the formation of the hexagonal H_{II} phase but also the complete phospholipid population appears to remain organized in extended bilayers up to at least 25 °C above the original transition. This bilayer spectrum, the low-field shoulder of which in fact is already visible also at lower R_i at 15 °C, is characterized, in line with the DEPE results, by a somewhat decreased chemical shift anisotropy of 38 ppm. The lack of sharp X-ray reflections (data not shown) again indicates the complete absence of H_{II} phase and points to no or irregular stacking of the bilayers, in agreement with the ob-

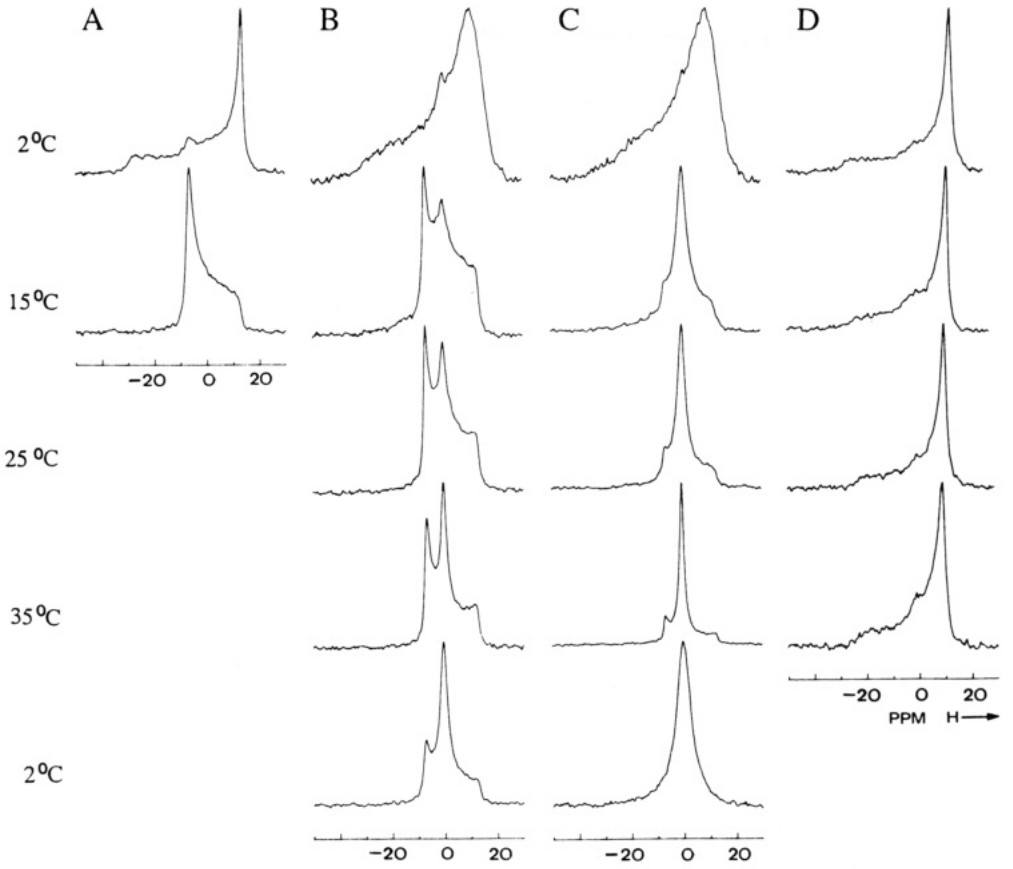

FIGURE 9: ^{31}P NMR spectra of DOPE–melittin samples of varying R_i. (A) Pure DOPE; (B) $R_i = 120$; (C) $R_i = 40$; (D) $R_i = 20$. The spectra at the bottom of the figure were recorded after heating to 35 °C and subsequent cooling to 2 °C.

servation on the melittin–DEPE system. Extremely high amounts of melittin appeared to be needed ($R_i < 2$) to solubilize the DOPE completely and to prevent any pelleting at 100000*g*.

Freeze–fracture was performed in order to get more information about the nature of the structure underlying the isotropic signal at higher R_i, an intermediate between the H_{II} phase of the pure lipid and the bilayer phase at $R_i = 20$. Quenching from room temperature results at $R_i = 40$ in electron microscopic images showing bilayer structure (Figure 10). On these bilayers, numerous, variably sized irregularities can be seen of a morphology similar to that shown in Figure 6D,E of Verkleij (1984), most likely representing sites of fusion between adjacent bilayers (fission stage; Verkleij, 1984). In these highly curved structures, lateral diffusion can cause further averaging of the ^{31}P chemical shift of the phosphates, leading to the observed isotropic NMR signal. At $R_i = 20$, mostly smooth bilayers are visualized, on which particles are relatively scarce.

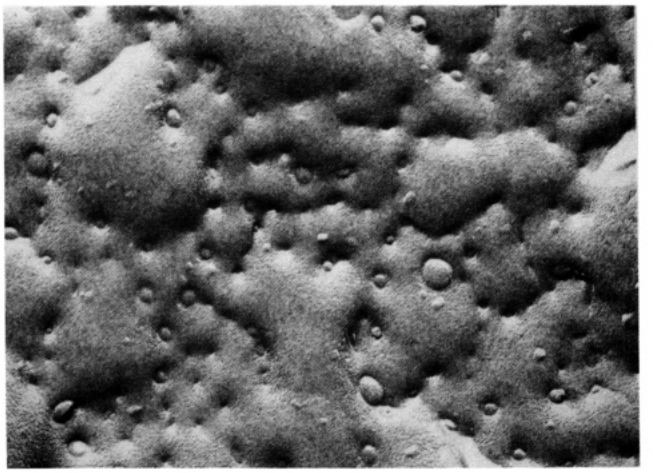

FIGURE 10: Electron microscopy of samples containing DOPE–melittin complex of $R_i = 40$, quenched from room temperature. Magnification: 55000×.

Discussion

The influence of melittin on the structure of phosphatidylethanolamines was studied and compared with the effect on an analogous phosphatidylcholine. First lipid–peptide binding was considered. Due to the formation of nonpelletable structures (small vesicles, disks, micelles) under certain conditions and turbidity problems in other cases, two different techniques had to be used for this goal. Analysis of the influence of the fluorescence data revealed that binding of melittin to the two lipid systems in the fluid state is remarkably similar in respect to both stoichiometry and affinity. At gel-state temperatures, however, considerable differences were observed. DEPE displayed a simple binding curve, easily interpretable due to a complete, R_i-independent, lipid pelleting. The lipid is able to bind less melittin when compared with the liquid-crystalline state, and the affinity is distinctly lower. Analysis of the data on melittin binding to gel-state DEPC is complicated by the appearance of nonpelletable structures, most likely disks (Dufourc et al., 1986), at relatively high R_i, for which a fluorescence maximum at an intermediate wavelength could be determined. Nevertheless, when the results of the two types of assays are combined, it is clear that the affinity of melittin for PC, unlike that for PE, is enhanced in the gel state.

The difference in the strength of the interaction with gel-state PC and PE is correlated with a different effect of melittin on the organization of the lipids. Whereas in PC the clearance

Table II: Compilation of Data Concerning the Lipid Structure-Modulating Activity of Melittin in Liquid-Crystalline Phospholipid Model Systems

lipid type	PC[a]	PE[b]	CL[c]	PA[d]	PG[d]
K_D (μM)[e]	1.5	1.7	0.016	0.02	0.013
stoichiometry[f]	25	25	4	2	4
structural effect of melittin at $R_i \sim 20$	vesicularization of liposomes and fusion of SUV to form closed bilayers of 1500-Å diameter	inhibition of H_{II} phase, formation of nonstacked bilayers	fusion of unilamellar vesicles, formation of lipidic particles[g]	formation of extended bilayers, induction of lipidic particles[g]	formation of large structures with high internal curvature
structural effect of melittin at $R_i \sim 4$	solubilization, micelle formation	turbidity decrease, at still lower R_i solubilization	H_{II}-phase formation	H_{II}-phase formation	formation of large irregularly stacked, probably inverted structures

[a] Egg PC/DPPC (Dufoucq et al., 1986); DEPC (this report). [b] DOPE/DEPE (this report). [c] Cardiolipin from bovine heart (Batenburg et al., 1987a). [d] Dioleoylphosphatidic acid and egg phosphatidylglycerol (Batenburg et al., 1987c). [e] Dissociation constant for binding to large structures based on fluorescence data; binding to micelles is not considered. [f] Phospholipid:peptide ratio; on basis of fluorescence data. [g] With "lipidic particles", the spherical, homogeneously sized type of particles are meant (Verkleij, 1984).

of the dispersion and the appearance in ^{31}P NMR of an isotropic signal at $R_i = 20$ confirm the bilayer fragmentation reported earlier (Dufourc et al., 1986), in PE, in contrast, all applied techniques demonstrate very little consequences of melittin presence for lipid organization. This lack of effect most likely originates from the much stronger inter-head-group interactions in PEs (Hauser et al., 1981), inhibiting a fragmentation of the bilayers. These stronger intermolecular forces could also be of importance for an explanation of the only moderate influence of melittin on the enthalpy of the L_β–L_α transition of DEPE. It is useful to compare here with other peptide–PE systems. In the gramicidin–DEPE system, the insensitivity of the transition toward the peptide was interpreted to be in favor of a more aggregated state of the peptide incorporated in PE (Killian & de Kruijff, 1985) as a consequence of the stronger cohesion of the lipids, and in glycophorin–PE and –PC, direct evidence for differences in aggregation of the protein has been presented (Taraschi et al., 1982; van Hoogevest et al., 1985).

The most striking, and for physiological situations most relevant, new observation, however, is the bilayer-stabilizing effect of melittin at temperatures where the pure PE adopts the H_{II} configuration. In DOPE at $R_i = 20$, the existence of extended bilayers is witnessed by ^{31}P NMR, up to temperatures far above the bilayer–H_{II} transition. At higher R_i, an isotropic signal was observed, which, however, by means of electron microscopy could also be related to bilayer structure. The observed curved structures, most likely interbilayer connections, in a situation apparently intermediate between the bilayer and the H_{II} organization are in line with the notion of the L_α–H_{II} transition being an interbilayer fusion event (Cullis et al., 1980). Complete H_{II}-phase inhibition and bilayer stabilization were also displayed by melittin in the DEPE system at 65 °C, but in contrast to DOPE at similar R_i, part of the lipid population, and at higher temperature the whole preparation, experienced isotropic motion. Most likely, here again high bilayer curvature is responsible for the isotropic ^{31}P NMR signal; it should also be realized that the slight differences with the DOPE system may be related to the higher temperature, leading to a faster diffusion and hence to a further averaging of the chemical shift anisotropy. Bilayer stabilization and H_{II}-phase inhibition in PE systems are new aspects of the action of melittin on phospholipid structure which need to be discussed in relation to earlier observations in other lipid systems.

Table II summarizes our current knowledge of the structural implications of the melittin–phospholipid interaction; for reasons of simplicity, the gel-state lipids are left out of consideration. It can be seen that melittin, in contrast to, for instance, the H_{II}-phase-inducing gramicidin (Killian et al., 1986) and the bilayer-stabilizing glycophorin (Taraschi et al., 1982, 1983), has effects as different as induction of H_{II} phase and H_{II}-phase inhibition, dependent on the lipid in question. In an earlier study, we demonstrated a deeper penetration of the tryptophan residue of melittin in cardiolipin model membranes when compared with PC vesicles, suggested to be due to electrostatic interactions. This deeper insertion, leading to an acyl chain spacing effect, was used to explain the inverted type of structures observed upon interaction of melittin with cardiolipin (Batenburg et al., 1987b); inversely, a convex curvature would then be induced in PC by a head-group spacing or "wedge" effect of more superficially inserted melittin molecules, eventually leading to micelles. This explanation is based on the shape–structure concept of lipid polymorphism (Cullis & de Kruijff, 1979), which predicts an inverted structure if the space occupied by the molecules in the acyl chain region exceeds that of the head-group region, and a micellar type of organization if the reverse situation applies.

If indeed the presence or absence of charge complementarity of lipid and peptide governs the penetration and thereby the structural consequences, as suggested also by results on the other negatively charged lipids (Table II), one would expect the penetration in PE to be similar to that in PC. The very similar binding stoichiometry and affinity for the two lipids (Table II) indeed suggest that the same forces account for the interaction. With respect to the resulting macroscopic organization, however, the phase preference of the lipid itself is evidently of equal importance. Apparently, in the PE–melittin system, the induction of micellar structure by the peptide is effectively counterbalanced by the H_{II} preference of the lipid, in a certain range of R_i values leading to the intermediate, lamellar structure. Similar bilayer organizations resulting from complementarity of molecular shapes have been reported for mixtures of lyso-PC and DOPE (Madden & Cullis, 1982) and of lyso-PC and cholesterol (Rand et al., 1975). The lyso-PC–gramicidin bilayer phase was explained likewise (Killian et al., 1983). All structure modulating effects of melittin thus can be explained on the basis of this single unifying shape–structure concept. For a full appreciation of the action of melittin, however, more detailed knowledge is necessary of the mode of insertion of melittin in the different lipid systems with respect to orientation and multimerization, which are still a matter of debate [see Batenburg et al. (1987b) and references cited therein]. The "inside-out tetramer" [Figure 10 of Vogel and Jähnig (1986)], put forward for zwitterionic lipid systems, could by its "hourglass" shape, for instance, well compensate the cone shape of the PE in a mixed bilayer.

Another point of interest will be the effect of melittin on membranes of mixed zwitterionic and negatively charged phospholipids. Table II indicates that the affinity of melittin for the charged lipid is 2 factors of magnitude higher; moreover, evidence on the basis of DSC results has been presented for a structural separation in mixed bilayers (Bernard et al., 1982). Hence, it can be anticipated that melittin and melittin-resembling peptides, for instance, the signal peptides, will induce organizations of concave rather than convex structure in natural lipid mixtures.

ACKNOWLEDGMENTS

We thank Dr. A. J. Verkleij and J. Leunissen-Bijvelt for performing the freeze–fracture electron microscopy and W. S. M. Geurts van Kessel for synthesis of the lipids. Dr. C. J. A. van Echteld and C. Mollay are kindly acknowledged for their preliminary experimental work in our department on melittin–PE systems.

Registry No. DEPC, 52088-89-8; DEPE, 16777-83-6; DOPE, 2462-63-7; DPPC, 2644-64-6; melittin, 20449-79-0.

REFERENCES

Batenburg, A. M., Hibbeln, J. C. L., Verkleij, A. J., & de Kruijff, B. (1987a) *Biochim. Biophys. Acta 903*, 142–154.

Batenburg, A. M., Hibbeln, J. C. L., & de Kruijff, B. (1987b) *Biochim. Biophys. Acta 903*, 155–165.

Batenburg, A. M., van Esch, J. H., Verkleij, A. J., Leunissen-Bijvelt, J., & de Kruijff, B. (1987c) *FEBS Lett. 223*, 148–154.

Bello, J., Bello, H. R., & Granados, E. (1982) *Biochemistry 21*, 461–465.

Bernard, E., Faucon, J.-F., & Dufourcq, J. (1982) *Biochim. Biophys. Acta 688*, 152–162.

Burnell, E. E., Cullis, P. R., & de Kruijff, B. (1980) *Biochim. Biophys. Acta 603*, 63–69.

Chupin, V., Killian, J. A., & de Kruijff, B. (1987) *Biophys. J. 51*, 395–405.

Comfurius, P., & Zwaal, R. F. A. (1977) *Biochim. Biophys. Acta 488*, 36–42.

Cullis, P. R., & de Kruijff, B. (1979) *Biochim. Biophys. Acta 559*, 399–420.

Cullis, P. R., de Kruijff, B., Hope, M. J., Najar, R., & Schmid, S. L. (1980) *Can. J. Biochem. 58*, 1091–1100.

Dasseux, J.-L., Faucon, J.-F., Lafleur, M., Pézolet, M., & Defourcq, J. (1984) *Biochim. Biophys. Acta 775*, 37–50.

de Kruijff, B., Cullis, P. R., Verkleij, A. J., Hope, M. J., van Echteld, C. J. A., & Taraschi, T. F. (1985a) in *The Enzymes of Biological Membranes* (Martonosi, A., Ed.) pp 131–204, Plenum, New York.

de Kruijff, B., Cullis, P. R., Verkleij, A. J., Hope, M. J., van Echteld, C. J. A., Taraschi, T. F., van Hoogevest, P., Killian, J. A., Rietveld, A., & van der Steen, A. T. M. (1985b) in *Progress in Protein–Lipid Interactions* (Watts, A., & de Pont, J. J. H. H. M., Eds.) pp 89–142, Elsevier, Amsterdam.

Dufourc, E., Faucon, J.-F., Fourche, G., Dufourcq, J., Gulik-Krzywicki, T., & Le Maire, M. (1986) *FEBS Lett. 201*, 205–209.

Dufourcq, J., & Faucon, J.-F. (1977) *Biochim. Biophys. Acta 467*, 1–11.

Dufourcq, J., Dasseux, J.-L., & Faucon, J.-F. (1984) *FEMS Symp. No. 24*, 127–138.

Dufourcq, J., Faucon, J.-F., Fourche, G., Dasseux, J.-L., Le Maire, M., & Gulik-Krzywicki, T. (1986) *Biochim. Biophys. Acta 859*, 33–48.

Fiske, C. M., & Subbarow, Y. (1925) *J. Biol. Chem. 66*, 375–389.

Freer, J. H., Birkbeck, T. H., & Bhakoo, M. (1984) *FEMS Symp. No. 24*, 181–189.

Habermann, E. (1972) *Science (Washington, D.C.) 177*, 314–322.

Hauser, H., Pascher, L., Pearson, R. H., & Sunbell, S. (1981) *Biochim. Biophys. Acta 650*, 21–51.

Hille, J. D. R., Donnê-op den Kelder, G. M., Sauve, P., de Haas, G. H., & Egmond, M. R. (1981) *Biochemistry 20*, 4068–4073.

Killian, J. A., & de Kruijff, B. (1985) *Biochemistry 24*, 7881–7890.

Killian, J. A., de Kruijff, B., van Echteld, C. J. A., Verkleij, A. J., Leunissen-Bijvelt, J., & de Gier, J. (1983) *Biochim. Biophys. Acta 728*, 141–144.

Killian, J. A., van den Berg, C. W., Tournois, H., Keur, S., Slotboom, A. J., van Scharrenburg, G. J. M., & de Kruijff, B. (1986) *Biochim. Biophys. Acta 857*, 13–27.

King, T. P., Sobotka, A. K., Kochoumian, L., & Lichtenstein, L. M. (1976) *Arch. Biochem. Biophys. 172*, 666–671.

Lavialle, F., Levin, I., & Mollay, C. (1980) *Biochim. Biophys. Acta 600*, 62–71.

Madden, T. D., & Cullis, P. R. (1982) *Biochim. Biophys. Acta 684*, 149–153.

Mollay, C. (1976) *FEBS Lett. 64*, 65–68.

Prendergast, F. G., Lu, J., Wei, G. J., & Bloomfield, V. A. (1982) *Biochemistry 21*, 6963–6971.

Rand, P. R., Pangborn, W. A., Purdas, A. D., & Tinker, D. O. (1975) *Can. J. Biochem. 53*, 189–195.

Rouser, G., Fleischer, S., & Yamamoto, A. (1975) *Lipids 5*, 494–496.

Seelig, J. (1978) *Biochim. Biophys. Acta 515*, 105–140.

Seelig, J., Borle, F., & Cross, T. A. (1985) *Biochim. Biophys. Acta 814*, 195–198.

Sessa, G., Freer, J. H., Colaccico, G., & Weissman, G. (1969) *J. Biol. Chem. 244*, 3575–3582.

Sitte, H., Edelmann, L., & Neumann, K. (1987) in *Cryotechniques in Biological Electron Microscopy* (Steinbrecht, R. A., & Zierold, K., Eds.) Springer-Verlag, West Berlin.

Taraschi, T. F., de Kruijff, B., Verkleij, A. J., & van Echteld, C. J. A. (1982) *Biochim. Biophys. Acta 685*, 153–161.

Taraschi, T. F., de Kruijff, B., & Verkleij, A. J. (1983) *Eur. J. Biochem. 129*, 621–625.

Terwillinger, T. C., & Eisenberg, d. (1982) *J. Biol. Chem. 257*, 6016–6022.

Valtersson, C., van Duijn, G., Verkleij, A. J., Chojnacki, T., de Kruijff, B., & Dallner, G. (1985) *J. Biol. Chem. 260*, 2742–2751.

van Deenen, L. L. M., & de Haas, G. H. (1964) *Adv. Lipid Res. 2*, 168–229.

van Dijck, P. W. M., de Kruijff, B., van Deenen, L. L. M., de Gier, J., & Demel, R. A. (1976) *Biochim. Biophys. Acta 455*, 576–587.

van Hoogevest, P., de Kruijff, B., & Garland, P. B. (1985) *Biochim. Biophys. Acta 813*, 1–9.

Verkleij, A. J. (1984) *Biochim. Biophys. Acta 779*, 43–63.

Vogel, H. (1981) *FEBS Lett. 134*, 37–42.

Vogel, H., & Jähnig, F. (1986) *Biophys. J. 50*, 573–582.

von Heijne, G. (1985) *J. Mol. Biol. 184*, 99–105.